Low-lying bands with different quadrupole deformation in ^{133}Nd

P. Petkov,[1,2] A. Dewald,[1] R. Peusquens,[1] S. Kasemann,[1] R. Krücken,[1,3] K. O. Zell,[1] P. von Brentano,[1] S. Lunardi,[4] D. Bazzacco,[4] F. Brandolini,[4] N. H. Medina,[4,5] P. Pavan,[4] C. M. Petrache,[4,6] C. Rossi-Alvarez,[4] G. de Angelis,[7] M. de Poli,[7] and D. R. Napoli[7]

[1]*Institut für Kernphysik der Universität zu Köln, D-50937 Köln, Germany*

[2]*Bulgarian Academy of Sciences, Institute for Nuclear Research and Nuclear Energy, 1784 Sofia, Bulgaria*

[3]*Wright Nuclear Structure Laboratory, Yale University, New Haven, Connecticut 06520*

[4]*Dipartimento di Fisica and INFN, Sezione di Padova, Padova, Italy*

[5]*Departamento de Fisica Nuclear, University of São Paulo, São Paulo, Brazil*

[6]*Dipartamento di Matematica e Fisica, University of Camerino, Camerino, Italy*

[7]*INFN, Laboratori Nazionali di Legnaro, Legnaro, Italy*

(Received 11 July 2000; published 5 December 2000)

The mean lifetimes of ten states in ^{133}Nd excited via the reaction ^{104}Pd(^{32}S,$2pn$) at $E_{^{32}\mathrm{S}}=135$ MeV were measured by means of the recoil-distance Doppler-shift method. The spectra obtained by setting a gate on the shifted component of a transition directly feeding the level of interest were analyzed within the framework of the differential decay-curve method. The intraband transition strengths are compared to calculations within the particle plus rotor model which reveal differences in the quadrupole deformations ϵ and γ of the bands studied.

DOI: 10.1103/PhysRevC.63.014304 PACS number(s): 21.10.Tg, 23.20.Lv, 27.60.+j

I. INTRODUCTION

The neutron-deficient ^{133}Nd has been the subject of numerous experimental investigations. Most of the works concentrated on the highly deformed (HD) band in this nucleus which is associated with an excitation based on the $i_{13/2}$ intruder orbital descending from above the $N=82$ shell gap. By means of Doppler-shift attenuation method (DSAM) and recoil-distance Doppler-shift (RDDS) lifetime measurements (see, e.g., Ref. [1]), it was established [2–5] that this band is characterized by a quadrupole deformation of $\beta_2=0.35$–0.40 ($\epsilon_2=0.33$–0.38). The low-lying [normal deformed (ND)] states have also been extensively explored [6,7]. The transitions feeding into them from the HD states were found in Refs. [8,9]. These studies resulted in a rather complex level scheme where the lowest quasineutron rotational bands of positive parity are the [404]7/2, [400]1/2, and [402]5/2 ones. The lowest negative-parity bands are characterized by the Nilsson quantum numbers [514]9/2 and [541]1/2. Below the band crossings, these structures are reasonably described by calculations [6,7] within the particle plus triaxial rotor model (PTRM) of Ref. [10].

Obviously, the observation of HD and ND states in the same nucleus is a manifestation of shape coexistence. The question arises whether all ND states are characterized by the same quadrupole deformation or on the contrary, their deformations differ. Hints for shape coexistence among the ND states were presented in Ref. [7]. They are based on the different values of the deformation parameters ϵ_2 and γ which provide the best PTRM fit of the level energies and γ-ray branching ratios. The DSAM lifetime measurements of Ref. [4] revealed that at higher spins the band [541]1/2 is characterized by a larger deformation ($\epsilon_2=0.28$) than the [404]7/2 ground-state band ($\epsilon_2=0.24$). To investigate the problem further, at lower spins, we have performed a coincidence RDDS experiment in order to determine lifetimes in some of the low-lying ND bands. Within our approach, the gates are set on transitions feeding the level of interest to eliminate the problem of the side feeding in the analysis. Thus, the first aim of the present work was to measure precisely electromagnetic transition strengths within the ND bands in ^{133}Nd. Our second aim was to perform new PTRM calculations and to obtain, on the basis of the comparison with the data, in particular with the newly obtained transition strengths, information on the quadrupole deformation (ϵ_2,γ) of each of the bands studied. Preliminary results of the present study were published in Ref. [11].

II. EXPERIMENT

The reaction ^{104}Pd(^{32}S,$2pn$) at a beam energy of $E=135$ MeV was used to populate excited states in ^{133}Nd. The beam was provided by the XTU tandem of the Laboratori Nazionali di Legnaro, Italy. The target and stopper foils were mounted in the Cologne plunger apparatus [12] in which the change of the target-to-stopper distance is realized by moving the target. The constancy of the preset distance is controlled by a feedback system using a piezoelectric device. More details about the plunger setup can be found in Ref. [12]. The target consisted of a 0.93 mg/cm^2 selfsupporting ^{104}Pd foil and the mean velocity $\langle v\rangle$ of the recoils when leaving it was 1.82(4)% of the velocity of light c. After the flight in vacuum, the recoils were stopped in a 12 mg/cm^2 gold foil. The deexciting γ rays were registered with the GASP array [13] in its configuration II (without the inner ball of BGO crystals). This array consists of 40 large volume Compton suppressed germanium detectors. The detectors which are positioned at approximately the same angle with respect to the beam axis can be grouped in seven rings. For the present coincidence RDDS experiment, the rings of interest are those where appreciable Doppler-shifts can be observed, i.e., ring 1 (mean angle with respect to the beam axis of 34.6°), ring 2 (59.4°), ring 6 (120.6°), and ring 7 (145.4°). Each of these rings consists of six detectors. Data were taken at 18 target-to-stopper distances x ranging from

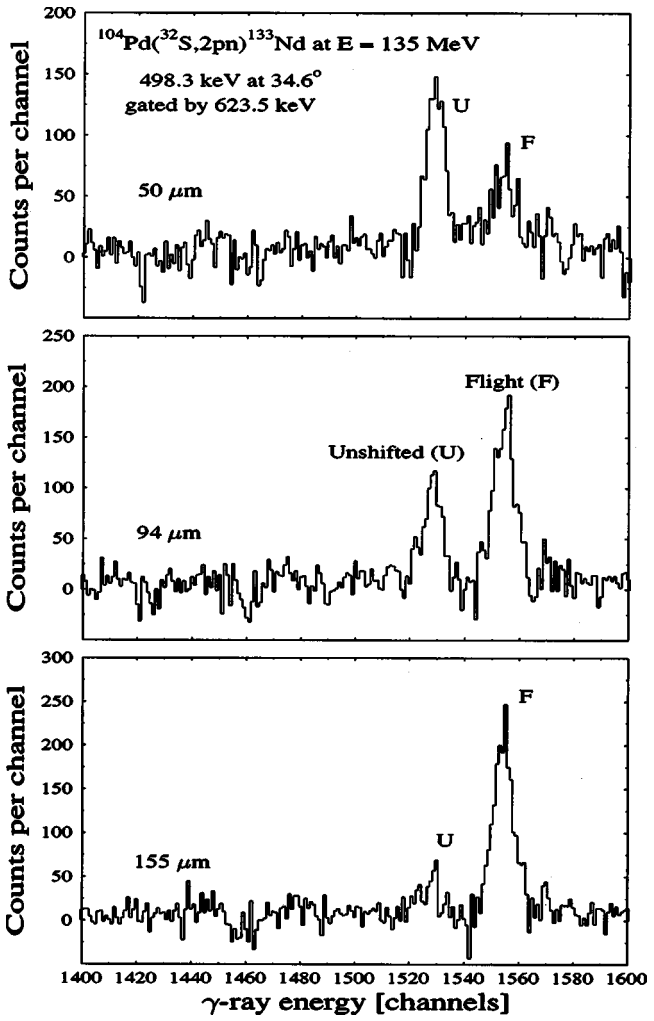

FIG. 1. Spectra measured at the indicated distances and obtained by setting a gate on the shifted component of the 623.5 keV transition which feeds the $15/2^-$ level of the [514]9/2 band (see also Fig. 3). The unshifted and flight peaks corresponding to the depopulating transition of 498.3 keV are clearly distinguished.

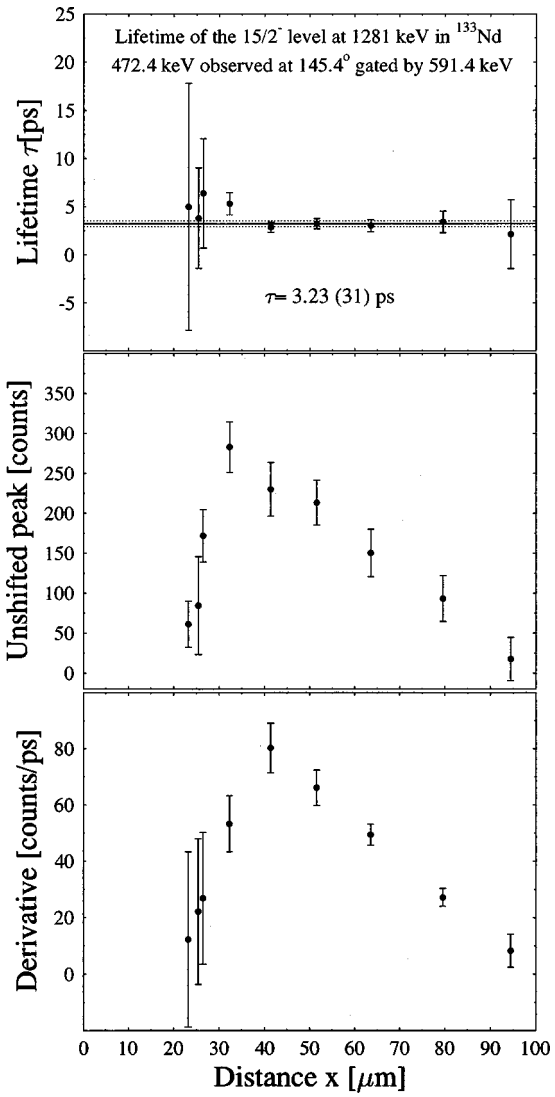

FIG. 2. Lifetime determination of the $I^\pi = 15/2^-$ level of the [541]1/2 band (see also Fig. 3) using data collected with the detectors of ring 7. The numerator and denominator on the right-hand side of Eq. (1) are shown in the middle and bottom of the figure, respectively. The $\tau(x)$ curve calculated with them is shown on top. The average value of the derived lifetime τ is displayed with its statistical uncertainties. See also text.

23 to 3000 μm. After corrections for energy shifts and gain matching of the detectors the data were sorted into 288 4k×4k γ-γ coincidence matrices. Each matrix accumulates coincident events where two γ rays are registered by detectors belonging to a particular two-ring combination at a given distance. A total of 1.7×10^9 unfolded doubles were collected. Normalization factors for the different distances were determined by using events corresponding to pairs of strong coincident transitions (see also Ref. [12]). Spectra for further analysis were obtained by setting a gate from above, on the shifted component of a transition feeding directly the level of interest. An example of such spectra at three different distances is shown in Fig. 1.

III. DATA ANALYSIS

The data were analyzed according to the differential decay-curve method (DDCM) developed in Refs. [14,15]. Referring the reader for more details to these works we present here only the main points. Let us consider a two-step cascade where the level *b* feeds via the transition *B* the level of interest *a* depopulated by the transition *A*. Both transitions can occur during the flight in vacuum (*F*) or after coming to rest (*U*). At every distance *x*, the lifetime τ_a of the level *a* can be derived using the following expression:

$$\tau_a(x) = \{B_F, A_U\} \Big/ \left(\langle v \rangle \frac{d}{dx} \{B_F, A_F\} \right), \qquad (1)$$

where the quantities in braces are coincidence events corresponding to a gate set on the flight (*F*) peak of the feeding transition *B*. The numerator represents the area of the unshifted (*U*) peak of the transition *A* in the gated spectrum. The denominator is the time-derivative of the area of the *F*

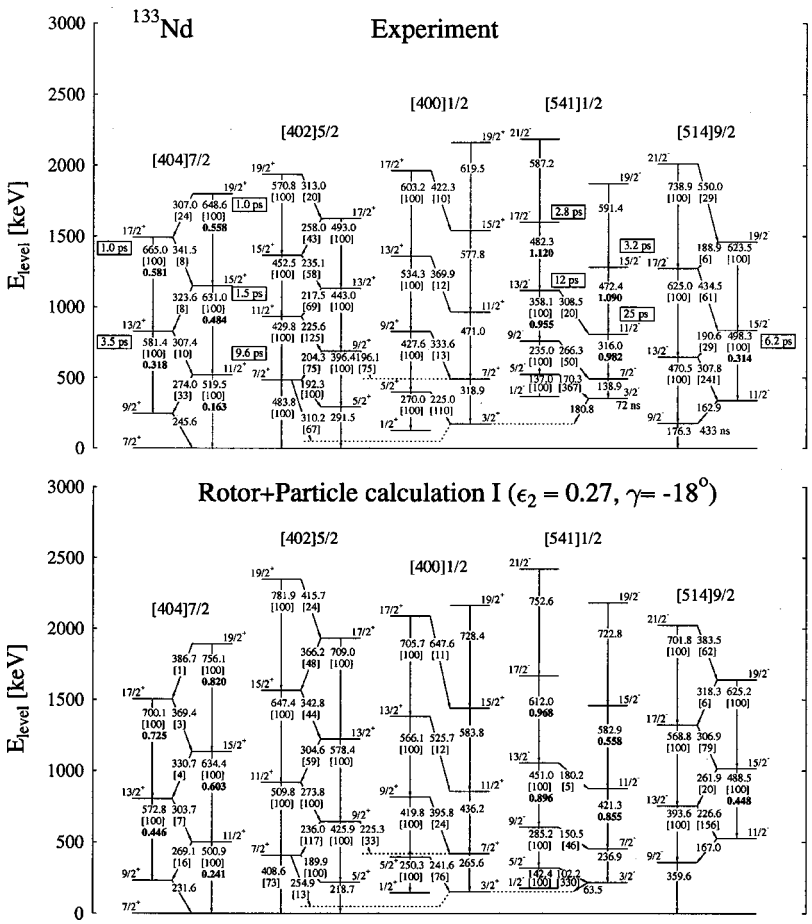

FIG. 3. Experimental partial level scheme of ^{133}Nd from Refs. [6,7] compared to PTRM calculations at the indicated quadrupole deformation. Lifetimes determined in the present work are displayed in framed boxes. Each level is characterized by the depopulating γ-ray transition energies and their relative branching ratios (in brackets and when relevant). Absolute $B(E2)$ transition strengths in e^2 b^2 are also displayed (in bold) in cases where they are experimentally known. See also text.

TABLE I. Lifetimes determined in the present work. In columns 1 and 2, the excitation energy and spin/parity of the investigated levels are shown, respectively. The depopulating γ-ray transition used in the data processing is displayed in column 3. The deduced lifetimes and their uncertainties in parentheses are presented in column 4. See also text and Fig. 3.

$E_{\rm lev}$ [keV]	I^π	E_γ [keV]	τ ($\Delta\tau$) [ps]
Band [541]1/2			
809	$11/2^-$	316.0	25.3(2.3)
1117	$13/2^-$	358.1	11.7(1.1)
1281	$15/2^-$	472.4	3.15(34)
1599	$17/2^-$	482.3	2.76(52)
Band [514]9/2			
838	$15/2^-$	498.3	6.18(53)
Band [404]7/2			
520	$11/2^+$	519.5	9.63(58)
827	$13/2^+$	581.4	3.46(34)
1151	$15/2^+$	631.0	1.54(24)
1492	$17/2^+$	665.0	0.99(35)
1799	$19/2^+$	648.6	1.01(22)

peak of the transition A obtained from the same spectrum. This derivative is determined by fitting piecewise with second order polynomials the areas $\{B_F, A_F\}$ as a function of the distance x and multiplying with the mean recoil velocity $\langle v \rangle$ the x derivative of the fitted curve. In the present analysis, at each distance the gates were set in four coincidence matrices where the gating detector rings are varied and the gated detector ring is kept fixed. The resulting spectra were summed up to increase the statistics. The lifetime is derived by fitting a straight line through the points of the $\tau(x)$ curve calculated according to Eq. (1) within the region of sensitivity where the numerator and denominator are reliable. Its final value is determined by averaging the results obtained using all analyzed data sets (whose maximal number is 4). We note that corrections of the data for relativistic, efficiency, and solid angle effects can be neglected in the present analysis. The deorientation effect was shown [16] to not affect the results of the analysis of coincidence RDDS measurements when it is performed in the framework of the DDCM. As an illustration, we show in Fig. 2 the determination of the lifetime of the $15/2^-$ level of the [541]1/2 band using gated spectra measured with the detectors positioned at 145.4° (ring 7).

IV. RESULTS

In total, ten lifetimes of excited states in ^{133}Nd were derived for the first time in the present work. They are displayed in framed boxes in Fig. 3 and presented in Table I.

TABLE II. Reduced electromagnetic transition probabilities $B(\sigma L)$ derived in this work. They are shown in units of $e^2\,\mathrm{b}^L$ for electric transitions and of $\mu_N^2\mathrm{b}^{L-1}$ for magnetic ones as well as in Weisskopf units (W.u.). The label of the investigated band is displayed in column 1. The level and depopulating transition energies are shown in the next two columns followed by the spin/parity of the initial (I_i^π) and final (I_f^π) levels. The multipolarity of the transitions σL as well as mixing ratios δ are displayed in column 6. The γ-ray branching ratios and δ values are taken from Ref. [7].

Band	E_{lev} [keV]	E_γ [keV]	I_i^π	I_f^π	σL	$B(\sigma L)$	$B(\sigma L)$ [W.u.]
Band [541]1/2	809	316.0	$11/2^-$	$7/2^-$	$E2$	$0.982^{+0.098}_{-0.082}$	243^{+24}_{-20}
	1117	358.1	$13/2^-$	$9/2^-$	$E2$	$0.955^{+0.099}_{-0.082}$	237^{+25}_{-20}
					$M1$	$2.38(83)\times10^{-2}$	$1.33(46)\times10^{-2}$
		308.5	$13/2^-$	$11/2^-$	$\delta=0.35(5)$		
					$E2$	$4.39(1.89)\times10^{-2}$	10.9(4.7)
	1281	472.4	$15/2^-$	$11/2^-$	$E2$	$1.090^{+0.132}_{-0.106}$	269^{+33}_{-26}
	1599	482.3	$17/2^-$	$13/2^-$	$E2$	$1.120^{+0.260}_{-0.178}$	277^{+64}_{-44}
Band [514]9/2	838	498.3	$15/2^-$	$11/2^-$	$E2$	$0.314^{+0.029}_{-0.025}$	78^{+7}_{-6}
		190.6	$15/2^-$	$13/2^-$	$M1$	$0.277^{+0.026}_{-0.022}$	$0.155^{+0.015}_{-0.012}$
Band [404]7/2	520	519.5	$11/2^+$	$7/2^+$	$E2$	$0.163^{+0.011}_{-0.009}$	41^{+3}_{-2}
		274.0	$11/2^+$	$9/2^+$	$M1$	$6.89^{+0.41}_{-0.39}\times10^{-2}$	$3.85^{+0.23}_{-0.22}\times10^{-2}$
	827	581.4	$13/2^+$	$9/2^+$	$E2$	$0.318^{+0.035}_{-0.029}$	79^{+9}_{-7}
		307.4	$13/2^+$	$11/2^+$	$M1$	$5.07^{+0.55}_{-0.45}\times10^{-2}$	$2.83^{+0.31}_{-0.25}\times10^{-2}$
	1151	631.0	$15/2^+$	$11/2^+$	$E2$	$0.484^{+0.089}_{-0.065}$	120^{+22}_{-16}
		323.6	$15/2^+$	$13/2^+$	$M1$	$8.29^{+1.53}_{-1.12}\times10^{-2}$	$4.63^{+0.85}_{-0.63}\times10^{-2}$
	1492	665.0	$17/2^+$	$13/2^+$	$E2$	$0.581^{+0.318}_{-0.152}$	144^{+79}_{-38}
		341.5	$17/2^+$	$15/2^+$	$M1$	$0.108^{+0.059}_{-0.028}$	$6.02^{+3.29}_{-1.56}\times10^{-2}$
	1799	648.6	$19/2^+$	$15/2^+$	$E2$	$0.558^{+0.155}_{-0.100}$	138^{+38}_{-25}
		307.0	$19/2^+$	$17/2^+$	$M1$	$0.368^{+0.103}_{-0.066}$	$0.206^{+0.058}_{-0.037}$

The relative uncertainties of the lifetimes are typically of the order of 10% and increase to 30% at higher spins due to the deteriorating statistics. The effect of the finite slowing down time of the recoils in the stopper (cf. Ref. [17]) is of importance for lifetimes below 2 ps and contributes also to the larger quoted errors of the shortest lifetimes. The elimination of the problem of the unknown feeding by gating from above ensures a high degree of reliability for the results.

The reduced transition probabilities $B(\sigma L)$ deduced from the lifetime data are presented in Table II. Thereby, known spectroscopic information on the γ-ray transitions depopulating the levels of interest was used (see caption to the table).

V. DISCUSSION

As already mentioned, the study of the level scheme of ^{133}Nd at low and moderate spins was completed in Refs. [6,7]. In these works, particle plus triaxial rotor model (PTRM) calculations were performed which allowed the association of the different observed bands with the excitation of the odd neutron in specific Nilsson orbitals. However, the lack of detailed data on electromagnetic transition strengths at low spin has limited the possibilities for comparison of these calculations with the experiment. In particular, the results of Ref. [6] leave undecided the question of whether the shape of ^{133}Nd is prolate or is characterized by deviations from axial symmetry. The conclusions of Ref. [7], where calculations of total Routhian surfaces (TRS) were also performed, indicate that some of the low lying bands ([541]1/2, [402]5/2, [404]7/2) are prolate while others ([514]9/2, [400]1/2) are characterized by a value of the asymmetry shape parameter $\gamma=-22°$. A value of the quadrupole deformation parameter $\epsilon_2=0.23$ was found to provide an optimal reproduction of data but a somewhat higher deformation $\epsilon_2=0.26$ was associated with the [541]1/2 intruder band originating from the $h_{9/2}$ subshell.

TABLE III. The energy $E_{2_1^+}$ of the even-even core and the pairing gap Δ used in the PTRM calculation II.

Band	[541]1/2	[514]9/2	[404]7/2
$E_{2_1^+}$ [MeV]	0.140	0.240	0.150
Δ [MeV]	1.061	1.065	1.084

These findings are a good starting point for a further study of ^{133}Nd within the framework of the PTRM with the aim to describe also the presently measured intraband transition strengths. For this purpose, we used the computer codes GAMPN, ASYRMO, PROBAMO, and E1PROBAM presented in Refs. [18,19] under the same limitations on the single-neutron orbitals involved as in Ref. [7] (15 for both parities

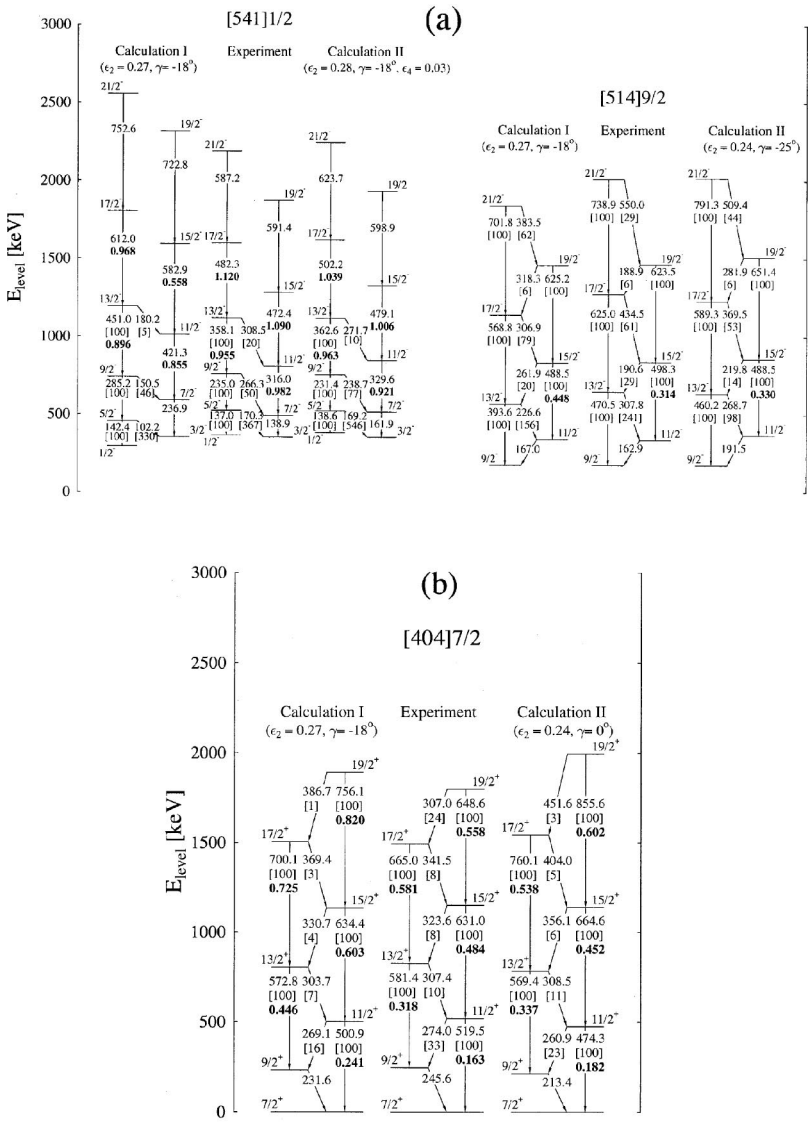

FIG. 4. (a) Low-lying negative-parity bands in ^{133}Nd compared to calculations I and II. The calculated band-head energies are set equal to the experimental ones. See also text. (b) The same as in (a), but for the [404]7/2 band.

in the vicinity of the Fermi level). First, the single-particle orbitals corresponding to the modified harmonic oscillator (MHO) potential are found for fixed quadrupole deformation (ϵ,γ). Then, they are coupled to a rigid (asymmetric in general) rotor to obtain wave functions characterized by a good angular momentum. Thereby, the attenuation ζ of the Coriolis interaction is treated as an adjustable parameter. The moments of inertia are also adjusted by the varying the energy $E_{2_1^+}$ of the 2_1^+ level of the even-even core while the pair correlations are treated within the BCS approach.

We performed two types of calculations. In the first variant (calculation I), the aim was a good overall description of the level energies and transition strengths. The results, compared to the experimental data in Fig. 3, are obtained with the optimal values of $\epsilon_2=0.27$, $\gamma=-18°$, $E_{2_1^+}=170$ keV, and $\zeta=0.7$. A value of $\Delta=1.122$ MeV was obtained by the BCS calculation for the paring gap. Thereby, the standard set [20] of Nilsson parameters κ and μ were used. A deviation from axial symmetry ($\gamma\neq 0$) was found to be essential for the correct reproduction of the relative positions of the positive-parity band heads. The agreement for the negative-parity band heads is worse but probably could be remedied by alternating the spin-orbital splitting of the $h_{11/2}$ and $h_{9/2}$ subshells. The calculated band-structures in Fig. 3 are easily identified with the corresponding experimental ones. However, a more detailed comparison reveals that some features are not sufficiently well reproduced. These are for instance the calculated level spacings which expand stronger than observed with increasing spin. The calculated absolute intraband transition strengths also deviate from the experimental ones. They are too large within the [404]7/2 and [514]9/2 bands and too small within the [541]1/2 band. The relative γ-ray branching ratios are in most of the cases reasonably described (for the calculation of the $M1$ transition strengths, the neutron g_s factor was reduced to 0.7 from its free value). It is interesting to mention that the PTRM calculation correctly reproduces the $E1$ transition strength from the $I^\pi=9/2^-$ level of the [514]9/2 band to the ground state (see Fig. 3). To the experimental value [6,7] of $B(E1,9/2^-\rightarrow 7/2^+)=2.5\times 10^{-9}\ e^2$ b corresponds a calculated value of

2.1×10^{-9} e^2 b. However, the experimental $B(E1,3/2^- \rightarrow 3/2^+)=1.4\times10^{-8}$ e^2 b transition strength from the $I^\pi=3/2^-$ level of the [541]1/2 band is somewhat underestimated by the calculation which yields a value of 6.5×10^{-10} e^2 b.

The results of calculation I, and especially the comparison of the obtained $B(E2)$ transition strengths with the experimental ones, indicate that the low-lying bands in ^{133}Nd are characterized by different quadrupole deformations. This is not surprising since the corresponding single-neutron orbitals depend in a very specific way on the deformation and therefore exercise different shape-driving force on the core. To shed more light on this problem, we have carried out a second calculation (II), where the properties of each band with measured intraband transition strengths were individually investigated as a function of the quadrupole deformation. While the attenuation of the Coriolis interaction was kept the same as in calculation *I* ($\zeta=0.7$), the parameters $E_{2_1^+}$ and Δ were also somewhat varied. Their optimal values are displayed in Table III. The final results are shown in the two parts of Fig. 4. In Fig. 4(a), the descriptions of the negative-parity bands obtained in calculations I and II are compared to the experimental data. Clearly, calculation II reproduces better the level energies and the absolute $B(E2)$ transition strengths although it is not superior with respect to the branching ratios. We note that in addition to the deviation from axial symmetry, some hexadecapole deformation ($\epsilon_4=0.03$) was found to be essential for reproducing the level staggering in the [541]1/2 band and especially the inversion of the $I^\pi=7/2^-,5/2^-$ and $I^\pi=3/2^-,1/2^-$ level pairs. The staggering in the [514]9/2 band is reasonably described by an ''increased'' value of $\gamma=-25°$ in comparison with calculation I ($\gamma=-18°$). This value is consistent with the result of the calculations presented in Ref. [7] ($\gamma=-22°\pm2°$). The [541]1/2 band is characterized by a relatively large deformation $\epsilon_2=0.28$ which correlates with the strong down-slopping behavior of this intruder orbital. A smaller deformation ($\epsilon_2=0.24$) characterizes the [514]9/2 band and the [404]7/2 band which is presented in Fig. 4(b). In the latter case, calculation II is for sure better with respect to the reproduction of the $B(E2)$ transition strengths and the branching ratios. A VMI treatment of the moment of inertia at prolate deformation ($\gamma=0°$) could certainly improve the description of the level spacings in the [404]7/2 ground-state band. Finally, we note the excellent agreement between the deformation parameters ϵ_2 derived in calculation II for the [404]7/2 and [541]1/2 bands and those determined experimentally in Ref. [4] for the same bands at higher spin. In practice, the two sets of parameters coincide (see Sec. I). These results confirm that the effect of shape coexistence persists up to higher spin in the bands considered.

VI. SUMMARY AND CONCLUSIONS

The lifetimes of ten excited states in ^{133}Nd were measured using the recoil-distance Doppler-shift method in coincidence mode which ensures the high reliability of the results. The data analysis was performed using the differential decay-curve method. The deduced electromagnetic transition strengths $B(\sigma\lambda)$ and other spectroscopic properties (level energies and branching ratios) of the low-lying bands are compared to calculations within the particle plus triaxial rotor model. This comparison reveals differences in the quadrupole deformations ϵ and γ of the investigated bands.

ACKNOWLEDGMENTS

This work was funded by the BMBF under Contract No. 06 OK 862 I (0). One of us (P.P.) is grateful for the kind hospitality of the University of Cologne. P.P. would like also to acknowledge the support provided by the Bulgarian National Research Foundation (BNRF) under Contract No. Ph.801.

[1] T.K. Alexander and J.S. Forster, Adv. Nucl. Phys. **10**, 197 (1978).

[2] S.M. Mullins, I. Jenkins, Y.-J. He, A.J. Kirwan, P.J. Nolan, J.R. Hughes, R. Wadsworth, and R.A. Wyss, Phys. Rev. C **45**, 2683 (1992).

[3] S.A. Forbes, G. Böhm, R.M. Clark, A. Dewald, R. Krücken, S.M. Mullins, P.J. Nolan, P.H. Regan, and R. Wadsworth, Z. Phys. A **352**, 15 (1995).

[4] F. Brandolini, N.H. Medina, D. Bazzacco, D. Bucurescu, M. Ionescu-Bujor, R.V. Ribas, C. Rossi-Alvarez, C.A. Ur, M. De Poli, G. de Angelis, G. Falconi, S. Lunardi, P. Pavan, R. Burch, and D. De Acuna, Phys. Rev. C **60**, 024310 (1999).

[5] F.G. Kondev, M.A. Riley, D.J. Hartley, T.B. Brown, R.W. Laird, M. Lively, J. Pfohl, R.K. Sheline, E.S. Paul, D.T. Joss, P.J. Nolan, S.L. Sheperd, R.M. Clark, P. Fallon, D.G. Sarantites, M. Devlin, D.R. LaFosse, F. Lerma, R. Wadsworth, I.M. Hibbert, N.J. O'Brien, J. Simpson, and D.E. Archer, Phys. Rev. C **60**, 011303(R) (1999).

[6] J.B. Breitenbach, J.L. Wood, M. Jarrio, R.A. Braga, J. Kormicki, and P.B. Semmes, Nucl. Phys. **A592**, 194 (1995).

[7] D. Bazzacco, F. Brandolini, G. Falconi, S. Lunardi, N.H. Medina, P. Pavan, C. Rossi-Alvarez, G. de Angelis, D. De Acuna, M. De Poli, D.R. Napoli, J. Rico, D. Bucurescu, M. Ionescu-Bujor, and C.A. Ur, Phys. Rev. C **58**, 2002 (1998).

[8] D. Bazzacco, F. Brandolini, R. Burch, A. Buscemi, C. Cavedon, D. De Acuna, S. Lunardi, R. Menegazzo, P. Pavan, C. Rossi-Alvarez, M. Sferrazza, R. Zanon, G. de Angelis, P. Bezzon, M.A. Cardona, M. De Poli, G. Maron, M.L. Mazza, D. Napoli, J. Rico, P. Spolaore, X.N. Tang, G. Vedovato, N. Blasi, I. Castiglioni, G. Falconi, G. LoBianco, P.G. Bizzeti, and R. Wyss, Phys. Lett. B **309**, 235 (1993).

[9] D. Bazzacco, F. Brandolini, R. Burch, S. Lunardi, E. Maglione, N.H. Medina, P. Pavan, C. Rossi-Alvarez, G. de Angelis, D. De Acuna, M. De Poli, J. Rico, D. Bucurescu, and C. Ur, Phys. Rev. C **49**, R2281 (1994).

[10] S.E. Larsson, G. Leander, and I. Ragnarsson, Nucl. Phys. **A307**, 189 (1978).

[11] R. Peusquens, A. Dewald, S. Kasemann, R. Krücken, H. Ties-

ler, K.O. Zell, P. von Brentano, P. Petkov, S. Lunardi, D. Bazzacco, F. Brandolini, N.H. Medina, P. Pavan, C.M. Petrache, C. Rossi-Alvarez, G. de Angelis, G. Maron, and D.R. Napoli (unpublished).

[12] A. Dewald, P. Sala, R. Wrzal, G. Böhm, D. Liebertz, G. Siems, R. Wirowski, K.O. Zell, A. Gelberg, P. von Brentano, P. Nolan, A.J. Kirwan, P.J. Bishop, R. Julin, A. Lampinen, and J. Hattula, Nucl. Phys. **A545**, 822 (1992).

[13] D. Bazzacco, Proceedings of the Interational Conference on Nuclear Structure at High Angular Momentum, Ottawa, 1992, Chalk River Report No. AECL 10613, p. 386.

[14] A. Dewald, S. Harissopulos, and P. von Brentano, Z. Phys. A **334**, 163 (1989).

[15] G. Böhm, A. Dewald, P. Petkov, and P. von Brentano, Nucl. Instrum. Methods Phys. Res. A **329**, 248 (1993).

[16] P. Petkov, Nucl. Instrum. Methods Phys. Res. A **349**, 289 (1994).

[17] P. Petkov, D. Tonev, J. Gableske, A. Dewald, T. Klemme, and P. von Brentano, Nucl. Instrum. Methods Phys. Res. A **431**, 208 (1999).

[18] I. Ragnarsson and P.B. Semmes, Hyperfine Interact. **43**, 425 (1988).

[19] P.B. Semmes (unpublished).

[20] T. Bengtsson and I. Ragnarsson, Nucl. Phys. **A436**, 14 (1985).